Faraday Discuss., 1994, **97**, 391–400

Time-resolved Studies of Photoinitiated Reactions in Binary and Larger $(N_2O)_m(HI)_n$ ($m \geqslant 1$, $n \geqslant 1$) Complexes‡

S. I. Ionov, P. I. Ionov and C. Wittig

Department of Chemistry, University of Southern California, Los Angeles, CA 90089-0482, USA

Under gas-phase conditions, reactions of fast hydrogen atoms with N_2O lead mainly to $OH(X\,^2\Pi) + N_2(X\,^1\Sigma)$ products *via* a 1,3 hydrogen-shift mechanism involving the HNNO intermediate. In complexes formed by using supersonic expansions, the reaction mechanism is less clear. In this paper, OH build-up times are reported for photoinitiated reactions in complexes of the form $(N_2O)_m(HI)_n$ with $m \geqslant 1$ and $n \geqslant 1$. The build-up times vary from many hundreds of fs under conditions that encourage the formation of larger complexes (*i.e.* the highest stagnation pressures) down to $\leqslant 100$ fs for the lowest stagnation pressures. We conclude that in binary complexes OH is produced on timescales below 100 fs. This rules out the participation of a long-lived intermediate such as $HNNO^\dagger$. Comparisons are made with the analogous CO_2–HI system, in which reactions in larger complexes either yield the same lifetimes as do binary complexes or are inhibited, presumably because of the relatively large $H + CO_2$ entrance channel barrier.

Reactive processes photoinitiated in weakly bound gaseous complexes have received considerable attention during the past decade.[1–4] The chemistries of such systems can be interesting and challenging in their own right and, in special cases, these environments can serve to help elucidate details of the corresponding gas-phase reactions. For example, the geometric structure of a parent complex can impose entrance channel constraints on important parameters such as the mutual orientations and impact parameters of reagents. Needless to say, such parameters play a major role in influencing overall reaction probabilities, branching ratios, and product-state distributions.[5–7] Another facet of chemical dynamics is made available when such reactions are initiated by short pulses, thereby forming reagents in close proximity at $t = 0$.[8–11] As a result, the dynamics become accessible to time-domain studies, *e.g.*, by probing the build-up of products as a function of the pump–probe delay.

Reactions (1) and (2) are among the most studied gas-phase reactions that involve four atoms:[12–36]

$$H + CO_2 \rightarrow OH + CO; \qquad \Delta H = 25.6 \text{ kcal mol}^{-1} \qquad (1)$$

$$H + N_2O \rightarrow OH + N_2; \qquad \Delta H = -62.8 \text{ kcal mol}^{-1} \qquad (2a)$$

$$\rightarrow HNNO^\dagger \rightarrow NNOH \rightarrow OH + N_2; \qquad \Delta H = -62.8 \text{ kcal mol}^{-1} \qquad (2b)$$

$$\rightarrow HNNO^\dagger \rightarrow NH + NO; \qquad \Delta H = 32.0 \text{ kcal mol}^{-1} \qquad (2c)$$

‡ Research supported by the US National Science Foundation.

where reaction (2*a*) represents direct hydrogen atom attack at the oxygen as opposed to the rearrangement path given in (2*b*). They have also been studied by photoinitiation within weakly bound complexes.[8–11,26,37–45] Specifically, initiation occurs by photodissociation of an HX (X = Cl, Br or I) moiety that is weakly bound to CO_2 or N_2O. Product state distributions,[17–23,33,40,44] the dependence of reaction probability of the 'collision' energy,[39] steric effects,[2,3,45] branching ratios,[26,31,32,44] and lifetimes of $HOCO^{\dagger}$ intermediates[8–11] have been reported in the literature.

With CO_2–HI complexes, reaction is believed to proceed through a vibrationally excited $HOCO^{\dagger}$ intermediate that dissociates *via* a unimolecular decomposition mechanism.[8–11] A significant steric effect has been reported,[2,3,45] and measured rates are in agreement with predictions made by using RRKM theory.[10,11] Though higher-than-binary complexes are known to be formed in the expansions, the measured OH production rates, $k(E)$, were shown to be insensitive to the degree of complexation, except that high concentrations of higher-than-binary complexes caused the signals to decrease. This suggests one or both of two possibilities: (i) Reaction is inhibited in higher complexes. This is not surprising since reaction (1) is quite endoergic and also displays a dynamical barrier when CO_2 is attacked by fast hydrogen atoms. Therefore, one might expect the added heat capacity of larger complexes to lessen the likelihood of reaction by slowing the hydrogen and/or altering its trajectories. (ii) In principle, OH deriving from higher-than-binary complexes could display the same build-up times as OH deriving from binary complexes. These caveats notwithstanding, agreement between experiment and theory is quite acceptable for this system.

Reaction (2) is more complicated. Fig. 1 shows relevant energies and pathways, taken from the recent *ab initio* calculations of Walch.[36] In accord with earlier theoretical work,[34,35] these calculations indicate two distinct channels leading to $OH + N_2$. The lowest entrance barrier is for hydrogen approaching the terminal nitrogen to form the $HNNO^{\dagger}$ intermediate, with reaction then proceeding *via* 1,3 migration. Alternatively, when hydrogen approaches the oxygen, reaction can take place directly, with interfragment repulsion setting in past the entrance barrier. As shown in Fig. 1, the barrier for this process is significantly greater than for $HNNO^{\dagger}$ formation.

With fast hydrogen atoms and gas-phase environments, both of the chemically distinct product channels listed above ($OH + N_2$ and $NH + NO$), as well as electronically excited $OH(A\,^2\Sigma)$, have been observed.[30,34,44] The mechanism for $OH(X\,^2\Pi)$ production has been shown to involve the formation of $HNNO^{\dagger}$ followed by a 1,3 hydrogen shift that leaves the N_2 product with an average vibrational excitation of *ca.* 20000 cm^{-1}.

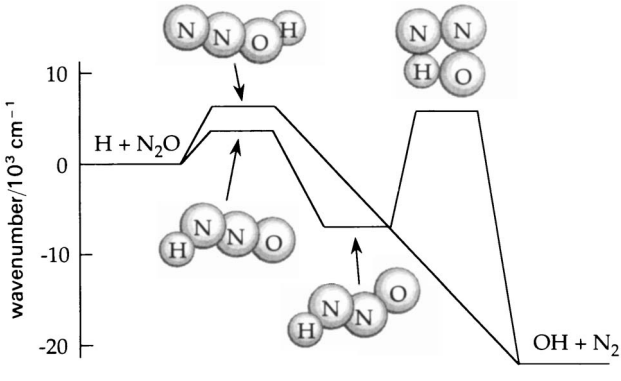

Fig. 1 Schematic representation of reaction paths leading to $OH(X\,^2\Pi)$, from ref. 36. Hydrogen attack at the oxygen involves a high entrance-channel barrier followed by exit-channel repulsion. Attack at the terminal nitrogen involves the HNNO intermediate followed by a 1,3 hydrogen shift. The endoergic path from HNNO to NH + NO is not shown.

This high degree of vibrational excitation is due to the large change in bond length in going from the 1,3 hydrogen shift transition state to the N_2 product (*i.e.* 1.23 Å *cf.* 1.10 Å). There was no evidence for the more geometrically direct process in which OH is formed by the hydrogen atom attacking the oxygen.

In complexes of the form N_2O–HX, there is direct spectroscopic evidence for hydrogen bonding to the oxygen when X = F or Cl.[46] However, with X = Br, the complex is inertially almost T-shaped, albeit with the hydrogen location unspecified.[46] Electronic structure calculations are in agreement with the experimental N_2O–HF and N_2O–HCl structures and suggest a modest degree of attraction between the hydrogen and oxygen for the case of N_2O–HBr.[46] For N_2O–HI, one can only guess: we expect large amplitude hydrogen zero-point fluctuations in an inertially T-shaped complex.

Photoinitiated reactions in N_2O–HI complexes have been shown to yield a much smaller (by an order of magnitude) [NH]/[OH] ratio than for the corresponding gas-phase reaction. There are a number of ways to rationalize this: (i) preferential attack at the oxygen; (ii) significant lowering of the effective 'collision energy' in the complex (*i.e.* more than in the analogous CO_2–HX system); (iii) removal of NH by HNI formation; (iv) involvement of a five atom highly excited intermediate *etc.*

If OH production rates from photoinitiated N_2O–HI complexes are measured with good temporal resolution (*e.g. ca.* 100 fs), it is possible to make at least qualitative statements about possible mechanisms. For example, if a long-lived intermediate is involved, this can be detected easily. Alternatively, if characteristic production times are found to be *ca.* 100 fs or less, it is hard to argue in favour of a statistical process, regardless of whether a 1,3 hydrogen shift mechanism is involved or not. With exceptional temporal resolution (*i.e.* 10s of fs) it may prove feasible to distinguish between reactions (2*a*) and (2*b*) but this is not within present state-of-the-art capability.

The above considerations presuppose that a binary complex serves as the precursor to the photoinitiated reaction. However, whenever binary complexes like N_2O–HI are formed in a supersonic expansion, larger complexes such as $(N_2O)_2HI$, $N_2O(HI)_2$ are also produced, though usually in smaller numbers. The presence of larger complexes is evident from mass spectrometer traces that show $(N_2O)_2HI^+$ and $N_2O(HI)_2^+$ cluster ions together with N_2OHI^+, N_2O^+, HI^+ *etc.* Though there is no doubt that larger complexes are present, a quantitative determination of the size distribution is formidable. Electron-impact ionization is a questionable tool since cracking patterns are not known and techniques such as IR spectroscopy are hard to implement in molecular beams for technical reasons.[46] Besides, a quantitative interpretation of IR data would require full rotational analysis for each species, which is not straightfoward, *e.g.* owing to spectral congestion.

The role of larger complexes in photoinitiated reactions is not clear *a priori*. Cluster geometries may favour reactions in one complex over another. Similarly, entrance channel barriers may vary somewhat, depending on surrounding species. The directions of these changes are not always obvious, even on theoretical grounds, and therefore experimental investigations are needed. For example, as stated above, in our time-resolved studies of photoinitiated reactions in CO_2–HI complexes,[11] we looked for signatures of reactions occurring in higher complexes. The presumption was that the photoinitiated reactions in higher complexes would proceed on longer timescales than their counterparts in binary systems. However, despite considerable effort, we were unable to detect a change in the product build-up time over a broad range of expansion conditions.

The present work is a report of time-resolved studies of photoinitiated reactions in N_2O–HI and larger complexes. Contrary to the case of CO_2–HX, product build-up times are seen to increase with the concentrations of N_2O and HI molecules in the sample being expanded. This is attributed to reactions in larger complexes. In the limit of low backing pressures, the product build-up time falls below our experimental

resolution, which is estimated as 50–100 fs. This observation does not justify an interpretation based solely on reaction 2(*a*). However, it eliminates the possibility that an intermediate lives more than 100 fs in the case of the N_2O–HI photoinitiated reaction.

Experimental

The temporal resolution of our apparatus has been improved by a factor of *ca.* 4 since our earlier studies.[10,11] This was achieved by compressing pulses that had been chirped in a fibre.[47] The ultrafast source shown schematically in Fig. 2 consists of a synchronously pumped dye laser followed by an optical fibre and a prism compressor. The laser operates on Kiton Red dye and a DQTCI saturable absorber, producing a 76 MHz train of 1 ps, 1 nJ pulses at 616 nm. The train is pre-amplified in a longitudinally pumped dye amplifier at 10 Hz prior to entering an 86 mm single-mode, polarization-preserving fibre (3M, 3.3 μm core diameter); optimal amplification gain is determined for each new fibre (typically × 100). Maintaining a constant intensity in the fibre is crucial for generating reproducible short pulses. Therefore, the amplification gain is adjusted periodically by tilting neutral-density filters in the pump line.

Pulses stretched in the fibre are compressed in a prism compressor[48] and amplified in a three-stage dye amplifier. The compressor consists of two 60° SF10 flint prisms arranged in a double-pass configuration (Fig. 2). This geometry provides coarse and fine tuning without affecting the pointing of the outgoing beam. The former is carried out by moving the back prism and reflector along the beam line, while the latter is achieved by moving the front prism in or out of the beam. The compressor is adjusted for minimal pulse duration on a saturable absorber (1 mm thick RG 695 Schott glass), which is located after the first amplification stage. The saturable absorber removes residual lobes and/or substrate that are inherent to fibre stretch–compression techniques. Additional dispersion accumulated in the next two amplification stages is compensated for in a second compressor consisting of four 60° SF10 prisms. Note that reflection losses in both compressors are negligible since the Brewster angle for flint glass is close to 60°. Typically, 0.5 mJ pulses are obtained at the output: an autocorrelation of amplified and compressed pulses is shown in Fig. 3.

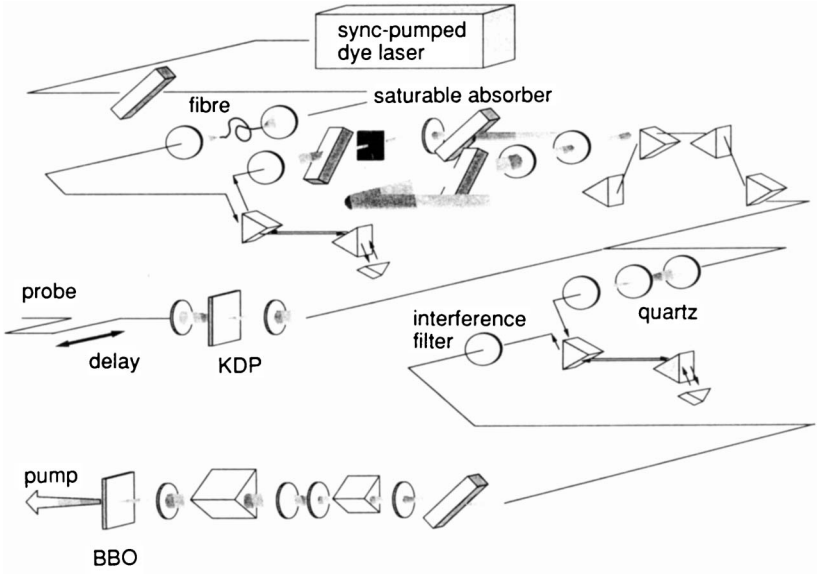

Fig. 2 Schematic representation of the ultrafast laser apparatus

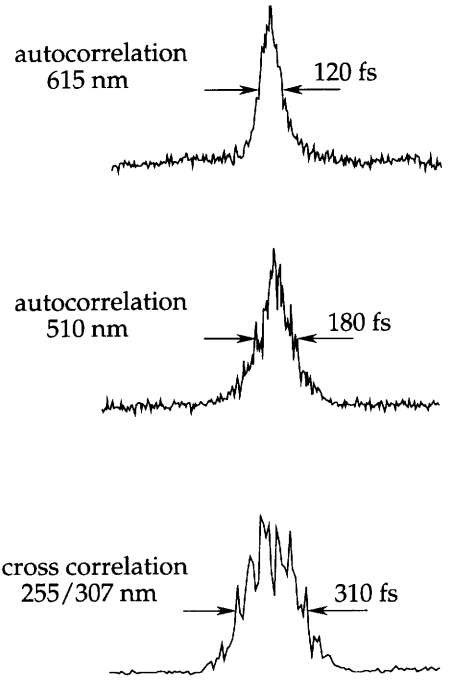

Fig. 3 Typical auto- and cross-correlations obtained under similar conditions

Approximately 80% of the 616 nm beam is split off by a broadband beam-splitter, frequency doubled in a 250 μm KDP crystal, and passed through a computer-controlled delay stage. This 308 nm ultrafast pulse is used as a probe. A 255 nm pump beam is obtained as follows. A small portion of the remaining 616 nm radiation is spatially selected from the 8 mm diameter beam by a 2 mm diaphragm and focussed into a 3 mm quartz plate, generating a supercontinuum. The supercontinuum is pre-chirped in a double-pass prism compressor, to compensate for subsequent group velocity dispersion in optical elements. The spectral band required for generating pump radiation is selected from the supercontinuum by an interference filter whose transmission is centred at 510 nm (200 cm^{-1} FWHM). The filtered supercontinuum is amplified to *ca.* 0.3 mJ in a three-stage Coumarin 503 dye amplifier. Its typical autocorrelation is presented in Fig. 3.

The 510 nm beam is doubled in a 100 μm thick BBO crystal, combined with the probe beam on a dichroic mirror, and focussed into a supersonic jet by a 50 cm focal length quartz lens. The jet is produced by expanding 0.67% HI–3.5% N_2O–95.8% He mixtures through a 1 mm × 0.1 mm slit nozzle at total pressures of 17–27 psi.† The effluent is probed by using a quadrupole mass spectrometer equipped with an electron-impact ionizer. N_2OHI^+ and larger cluster ions are observed. By reducing stagnation pressures from 23 to 19 psi, the concentrations of $(N_2O)_2HI^+$ and $N_2O(HI)_2^+$ relative to N_2OHI^+ drop from 22% and 22% to 17% and 17%, respectively; however, we are not able to eliminate them completely while retaining sufficient binary complexes.

The 255 nm pump pulse initiates reactions by photolysing the HI moiety in $(N_2O)_n(HI)_m$ complexes, while the 308 nm beam probes the outcome by exciting laser-

† 1 psi = 6894.76 Pa.

induced fluoresecence (LIF) in the OH $A\,^2\Sigma \leftarrow X\,^2\Pi$ system after a controlled delay. LIF is collected by an F/1 quartz condenser and focussed onto a PMT (RCA 1034). To minimize backgound from various non-linear processes, an interference filter with transmission centred at 307 nm (10 nm bandpass) is positioned between the collection optics and the PMT. Though the filter attenuates the signal by a factor of 4, its use is imperative for distinguishing LIF from background. Typical signals are 0.2–0.5 counts per laser pulse.

Simultaneously with the LIF measurements, the pump and probe energies are measured by Si photodiodes and a pump–probe cross-correlation is obtained by difference-frequency generation. For these purposes, a Fresnel reflection is taken from the front surface of the entrance window, which is oriented at the Brewster angle for the opposite polarization. The reflected beams are focussed into a 90 μm BBO crystal, and the resulting difference frequency at 1.5 μm is detected by a Ge photodiode after passing through a 1 mm RG 610 Schott filter. In order to compensate for different group velocity dispersions in the LIF and cross-correlation channels, a tilted quartz plate is placed

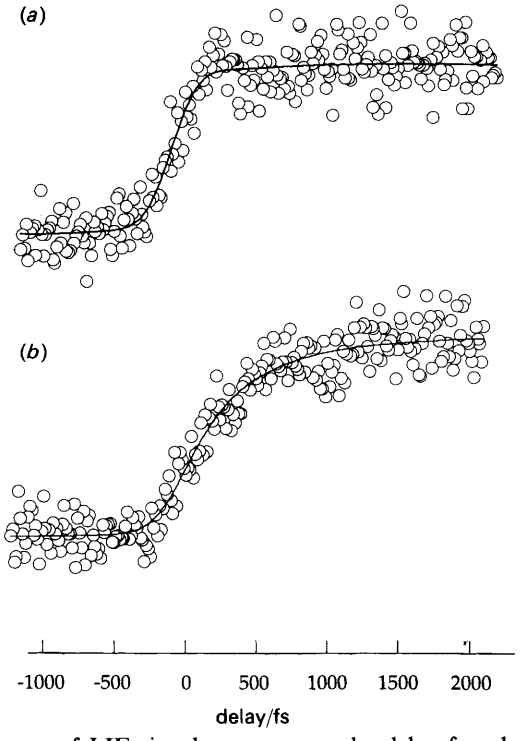

Fig. 5 Representative scans of LIF signal *vs.* pump–probe delay for photoinitiated reactions in $(N_2O)_n(HI)_m$ complexes with 0.67% HI and 3.5% NO_2 at (*a*) 19 psi; $\tau = 50$ fs and (*b*) 27 psi; $\tau = 350$ fs; $\lambda_{pump} = 255$ nm; $\lambda_{probe} = 308$ nm

$\Delta\omega_{FT}$. In our case, $\Delta\omega \geqslant 3\Delta\omega_{FT}$. Therefore we assume that the signal is given by:

$$S(t) = \text{const} \times \int_{-\infty}^{t} \mathrm{d}sR(s)N(t-s) \tag{3}$$

where $R(s)$ is the experimental pump–probe cross-correlation and $N(t)$ models product build-up. Lacking a better guess, we assume $N(t) = 1 - \exp(-t/\tau)$, where τ is an adjustable parameter representing the lifetime of reaction intermediates.

To verify the applicability of the rate approach, HOOH was photodissociated *via* a repulsive potential surface (Fig. 4). This is known to proceed on the timescale of a

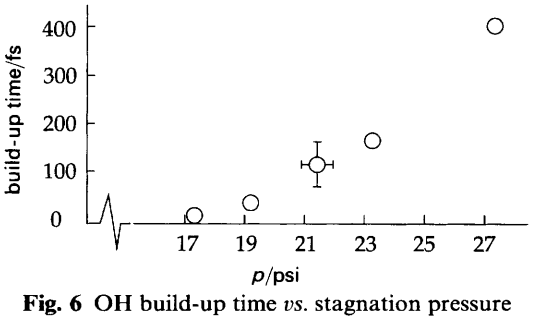

Fig. 6 OH build-up time *vs.* stagnation pressure

vibrational period,[50] *i.e.* instantaneous at the present temporal resolution. The best fit of the data (solid line) gives $\tau = 10$ fs. As shown in the figure, the fit is quite satisfactory. Traces of similar quality were acquired consistently throughout the course of the measurements; all gave lifetimes $\leqslant 60$ fs.

Fig. 5 shows typical dependences of LIF photon count *vs.* pump–probe delay for photoinitiated reactions in $(N_2O)_n(HI)_m$ complexes. Scans were acquired over periods of 3–5 h, depending on the magnitude of the signal. As is evident from a visual comparison, higher stagnation pressures give rise to slower OH build-up times. This trend is supported by computer fits of the data by using eqn. (3). The fits are shown as solid lines in Fig. 5, and the corresponding build-up times are plotted *vs.* stagnation pressure in Fig. 6. Each point is an average of three to five measurements taken on different days. It has not been possible to acquire data at lower stagnation pressures because of small LIF signals.

Discussion

As is evident from the increase in product build-up times, larger $(N_2O)_n(HI)_m$ complexes participate in photoinitiated reactions at higher stagnation pressures. Indeed, higher pressures favour the formation of larger complexes due to the increased collision frequency and a decrease in the asymptotic temperature. This is confirmed qualitatively by mass-spectrometric probes of beam composition, which indicate a decrease in the $(N_2O)_2HI^+$ and $N_2O(HI)_2^+$ signals relative to the N_2OHI^+ signal, *i.e.* from 22% and 22% to 17% and 17%, respectively, as the stagnation pressure is lowered from 23 to 19 psi.

Because there are more degrees of freedom in larger complexes, product appearance lifetimes are expected to be longer than for binary complexes. When the stagnation pressure, p, is lowered, the size distribution of $(N_2O)_n(HI)_m$ complexes shifts towards lower values of n and m, and at sufficiently low pressures, only binary complexes are present, together with the parent molecules. Complexes of the form $(HI)_x$ and $(N_2O)_y$ are of no concern since they do not yield OH. Thus, assuming a non-zero reaction probability for binary complexes, the $p = 0$ limit of product build-up times represents N_2O–HI.

There is insufficient signal at the lowest pressures to permit an unambiguous extrapolation to $p = 0$. However, it seems reasonable to assume that $\tau(p)$ does not increase as $p \rightarrow 0$ and that build-up times for the higher complexes are larger than those for binary complexes. In this case, OH appearance lifetimes for photoexcited N_2O–HI complexes are below our temporal resolution, which is estimated as 50–100 fs.

In experiments such as those reported here, in which product build-up is recorded as a function of pump–probe delay, the experimental time resolution is limited fundamentally by the LIF detection process. Specifically, since $OH(A\ ^2\Sigma)$ is known to be quenched efficiently by N_2, detection is inhibited at small interfragment distances. This can result in an apparent delay in the build-up of OH product. For example, for an OH–N_2 speed of 2×10^5 cm s^{-1}, the interfragment distance increases by only 2 Å.in 100 fs. Therefore, it may not be possible to observe significantly faster build-up times with the present experimental approach.

Changes in cluster ion signals are considerably less dramatic than the product build-up times presented in Fig. 6. This suggests that electron-impact ionization is unreliable for determining cluster composition. Cracking patterns are unknown and similar distributions of binary and tertiary cluster ions might be observed for different neutral cluster distributions.

The direct reaction of fast hydrogen atoms with N_2O, *i.e.* proceeding *via* reaction (2*a*), should yield products on the timescale of a vibrational period. With the present temporal resolution, such rise-times would appear instantaneous, in accord with the experimental observations. However, indirect reactions are hard to rule out on the basis of lifetimes alone, since they may also result in short OH production times. For example,

RRKM estimates of HNNO† lifetimes give *ca.* 100 fs for our conditions.[51] Estimates of such short decomposition lifetimes provide qualitative guidance, but cannot be assumed to be reliable quantitatively, since chemical reaction and intramolecular vibrational redistribution (IVR) may occur on comparable timescales.

Lengthening of the product rise-time with the concentrations of higher complexes suggests an indirect reaction mechanism in larger complexes. However, it does not clarify the nature of the intermediates. Geometrical constraints in larger complexes may be different from those in binary species. For example, one might argue that a larger number of entrance channel orientations and impact parameters are available with larger clusters. In this respect, reactions in larger complexes are closer to those in the gas phase than their binary counterparts. In accord with our experimental observations, lifetimes of the intermediate are expected to increase with cluster size, since a portion of the available energy is taken by the neighbouring species.

Finally, it is interesting to compare photoinitiated reactions in N_2O–HI (and larger) complexes with our previous studies of CO_2–HI.[10,11] With the latter, no change in product build-up time was observed over a broad range of expansion conditions. Moreover, the intensity of the OH LIF signals decreased when the CO_2 and HI concentrations were increased considerably in the sample being expanded. Altogether, these observations suggest that OH build-up times either depend little on the size of the complex or that reactions are inhibited in the larger $(CO_2)_m(HI)_n$ complexes. With respect to the latter, the difference between the two systems can be rationalized by considering the energetics of the $H + N_2O \rightarrow OH + N_2$ and the $H + CO_2 \rightarrow OH + CO$ reactions. The former has relatively low entrance channel barriers [*i.e.* 10.3 and 18.0 kcal mol^{-1} for reactions (2*a*) and (2*b*),[36] see Fig. 1] compared with the latter, in which $\Delta H = 25.6$ kcal mol^{-1}.[15,16,24] Furthermore, for fast hydrogen atoms, the probability of reaction (1) is known to be small just above the energy threshold and its variation with centre-of-mass (cm) collision energy is pronounced.[39] It is likely that in larger complexes the hydrogen atoms lose some of their initial energy, and this may affect their reactivity with CO_2 much more than that with N_2O.

Outlook

To gain further insight into the nature of photoinitiated reactions in binary and larger complexes, additional experiments are desirable. First, it would be helpful to select a specific cluster size by vibrational excitation. Reactions could then be initiated in tagged species by UV photons that do not act on untagged species. Such experiments require at least some knowledge of the IR spectra of $(N_2O)_n(HI)_m$ complexes. Secondly, it would be instructive to study the real-time build-up of $NH(X\,^3\Sigma)$ deriving from binary complexes, since NH derives from an HNNO intermediate. If different risetimes were found for the NH and OH products, it could assist in assignments of direct and/or indirect mechanisms to the corresponding channels.

The authors acknowledge useful discussions with A. H. Zewail, C. Jaques and E. Boehmer.

References

1 M. Takayanagi and I. Hanazaki, *Chem. Rev.*, 1991, **91**, 1193.
2 S. K. Shin, Y. Chen, S. Nickolaisen, S. W. Sharpe, R. A. Beaudet and C. Wittig, in *Advances in Photochemistry*, ed. D. Volman, G. Hammond and D. Neckers, Wiley, New York, 1991, vol. 16, p. 249.
3 Y. Chen, G. Hoffmann, S. K. Shin, D. Oh, S. Sharpe, Y. P. Zeng, R. A. Beaudet and C. Wittig, in *Advances in Molecular Vibrations and Collision Dynamics*, JAI Press, Greenwich, 1992, vol. 1, p. 187.
4 S. K. Shin, Y. Chen and C. Wittig, in *Topics in Applied Physics*, Springer-Verlag, Berlin, 1992, vol. 70, p. 57.

5 R. D. Levine and R. B. Bernstein, *Molecular Reactions Dynamics and Chemical Reactivity*, Oxford, New York, 1987.
6 S. Stolte, in *Atomic and Molecular Beam Methods*, ed. G. Scoles, Oxford, New York, 1987, vol. 1, ch. 25.
7 P. R. Brooks, *Science*, 1976, **193**, 1.
8 N. F. Scherer, L. R. Khundkar, R. B. Bernstein and A. H. Zewail, *J. Chem. Phys.*, 1987, **87**, 1451.
9 N. F. Scherer, C. Sipes, R. B. Bernstein and A. H. Zewail, *J. Chem. Phys.*, 1990, **92**, 5239.
10 S. I. Ionov, G. A. Brucker, C. Jaques, L. Valachovic and C. Wittig, *J. Chem. Phys.*, 1992, **97**, 9486.
11 S. I. Ionov, G. A. Brucker, C. Jaques, L. Valachovic and C. Wittig, *J. Chem. Phys.*, 1993, **99**, 6553.
12 G. A. Oldershaw and D. A. Porter, *Nature (London)*, 1969, **223**, 490.
13 R. E. Tomalesky and J. E. Sturm, *J. Chem. Soc., Faraday Trans. 2*, 1972, **68**, 1241.
14 C. R. Quick Jr., R. E. Weston Jr. and G. W. Flynn, *Chem. Phys. Lett.*, 1981, **83**, 15.
15 J. Brunning, D. W. Derbyshire, I. W. M. Smith and M. D. Williams, *J. Chem. Soc., Faraday Trans. 2*, 1988, **84**, 105.
16 M. J. Frost, P. Sharkey and I. W. M. Smith, *Faraday Discuss., Chem. Soc.*, 1991, **91**, 305.
17 K. Kleinermanns and J. Wolfrum, *Laser Chem.*, 1983, **2**, 339.
18 K. Kleinermanns and J. Wolfrum, *Chem. Phys. Lett.*, 1984, **104**, 157.
19 K. Kleinermanns, E. Linnebach and J. Wolfrum, *J. Phys. Chem.*, 1985, **89**, 2525.
20 A. Jacobs, M. Wahl, R. Weller and J. Wolfrum, *Chem. Phys. Lett.*, 1989, **158**, 161.
21 C. Wittig, G. Hoffmann, Y. Chen, H. Iams and D. Oh, *J. Chem. Soc., Faraday Trans. 2*, 1989, **85**, 1292.
22 S. Nickolaisen, H. E. Cartland and C. Wittig, *J. Chem. Phys.*, 1992, **96**, 4378.
23 J. K. Rice, Y. C. Chung and A. P. Baronavski, *Chem. Phys. Lett.*, 1990, **167**, 151.
24 J. C. Schatz, M. S. Fitzcharles and L. B. Harding, *Faraday Discuss., Chem. Soc.*, 1987, **84**, 359.
25 K. Kudla, G. C. Schatz and A. F. Wagner, *J. Chem. Phys.*, 1991, **95**, 1635.
26 G. Hoffmann, D. Oh, H. Iams and C. Wittig, *Chem. Phys. Lett.*, 1989, **155**, 356.
27 G. Hoffmann, D. Oh and C. Wittig, *J. Chem. Soc., Faraday Trans. 2*, 1989, **85**, 1141.
28 G. Dixon-Lewis and D. J. Williams, in *Gas-phase Combustion, Comprehensive Chemical Kinetics*, ed. C. H. Bamford and C. F. H. Tipper, Elsevier, Amsterdam, 1977, vol 17.
29 W. E. Hollingworth, J. Subbiah, G. W. Flynn and R. F. Weston Jr., *J. Chem. Phys.*, 1985, **82**, 2295.
30 P. Marshall, T. Ko and A. Fontijn, *J. Phys. Chem.*, 1989, **93**, 1922.
31 K. Yamasaki, S. Okada, M. Koshi and H. Matsui, *J. Chem. Phys.*, 1991, **95**, 5087.
32 J. D. Mertens, A. Y. Chang, R. K. Hanson and C. Bowman, *Int. J. Chem. Kinet.*, 1991, **23**, 173.
33 D. Patel-Misra and P. J. Dagdigian, *J. Phys. Chem.*, 1992, **96**, 3232.
34 P. Marshall, A. Fontijn and C. F. Melius, *J. Chem. Phys.*, 1987, **86**, 5540.
35 T. Fueno, M. Fukuda and K. Yokoyama, *Chem. Phys.*, 1988, **124**, 265.
36 S. P. Walch, *J. Chem. Phys.*, 1993, **98**, 1170.
37 S. Buelow, G. Radhakrishnan and C. Wittig, *J. Phys. Chem.*, 1987, **91**, 5409.
38 J. Rice, G. Hoffmann and C. Wittig, *J. Chem. Phys.*, 1988, **88**, 2841.
39 Y. Chen, G. Hoffmann, D. Oh and C. Wittig, *Chem. Phys. Lett.*, 1989, **159**, 426.
40 H. Ohoyama, M. Takayanagi, T. Nishiya and I. Hanazaki, *Chem. Phys. Lett.*, 1989, **162**, 1.
41 G. Hoffmann, D. Oh, Y. Chen, Y. M. Engel and C. Wittig, *Israel J. Chem.*, 1990, **30**, 115.
42 S. W. Sharpe, Y. P. Zeng, C. Wittig and R. A. Beaudet, *J. Chem. Phys.*, 1990, **92**, 943.
43 S. K. Shin, C. Wittig and W. A. Goddard III, *J. Phys. Chem.*, 1991, **95**, 8048
44 E. Böhmer, S. K. Shin, Y. Chen and C. Wittig, *J. Chem. Phys.*, 1992, **97**, 2536.
45 S. K. Shin, Y. Chen, D. Oh and C. Wittig, *Philos. Trans. R. Soc., London Ser. A*, 1990, **332**, 361.
46 Y. P. Zeng, S. W. Sharpe, D. Reifschneider, C. Wittig and R. A. Beaudet, *J. Chem. Phys.*, 1990, **93**, 183.
47 W. J. Tomlinson, R. H. Stolen and C. V. Shank, *J. Opt. Soc. Am. B: Opt. Phys.*, 1984, **1**, 139.
48 R. L. Fork, O. E. Martinez and J. P. Gordon, *Opt. Lett.*, 1984, **9**, 150.
49 H. Okabe, *Photochemistry of Small Molecules*, Wiley, New York, 1978.
50 R. Schinke, *Photodissociation Dynamics*, Cambridge University Press, Cambridge, 1993.
51 P. I. Ionov, S. I. Ionov and C. Wittig, unpublished results.

Paper 4/00269E; *Received* 11*th January*, 1994